Inorganic Materials, Vol. 41, No. 5, 2005, pp. 460–467. Translated from Neorganicheskie Materialy, Vol. 41, No. 5, 2005, pp. 540–547.

Preparation of Nanocrystalline Alumina under Hydrothermal Conditions

O. V. Al'myasheva, E. N. Korytkova, A. V. Maslov, and V. V. Gusarov

Grebenshchikov Institute of Silicate Chemistry, Russian Academy of Sciences, ul. Odoevskogo 24/2, St. Petersburg, 199155 Russia

e-mail: gusarov@isc.nw.ru

Received December 25, 2003

Abstract—Thermodynamic analysis of phase equilibria in the Al_2O_3–H_2O system at temperatures from 120 to 380°C and pressures from 1 to 70 MPa is carried out, and the dehydration of aluminum hydroxide under hydrothermal conditions is studied experimentally. The results indicate that γ-AlOOH (boehmite), which commonly appears in experimental phase diagrams, is a nonequilibrium phase in these temperature and pressure ranges. The dehydration rate and mechanism are shown to strongly depend on the crystallinity of the parent aluminum hydroxide and the pressure in the hydrothermal system.

INTRODUCTION

Alumina exists in a wide variety of polymorphs [1–20]. At the same time, the only equilibrium alumina polymorph is corundum, α-Al_2O_3 (Fig. 1) [1–24]. Note that the decomposition of salts, hydroxides, and oxyhydroxides in air at normal pressure and also crystallization from the melt may yield different alumina polymorphs, depending on the thermal history and chemical form of the starting materials [1–20]. The main product of hydrothermal crystallization is α-Al_2O_3 (Fig. 2) (see, e.g., [21]).

At the same time, various (and sometimes contradictory) data have been reported in the literature as to the formation of alumina through the dehydration of aluminum hydroxides (oxyhydroxides) under hydrothermal conditions. According to Laubengayer and Weiss [22], corundum is a stable phase above 450°C under hydrothermal conditions. To establish the stability regions of crystalline phases in the Al_2O_3–H_2O system, Erwin and Osborn [23] mapped out *p*–*t* phase diagrams. Using a hydrothermal process at temperatures from 320 to 400°C and water vapor pressures from 1.5

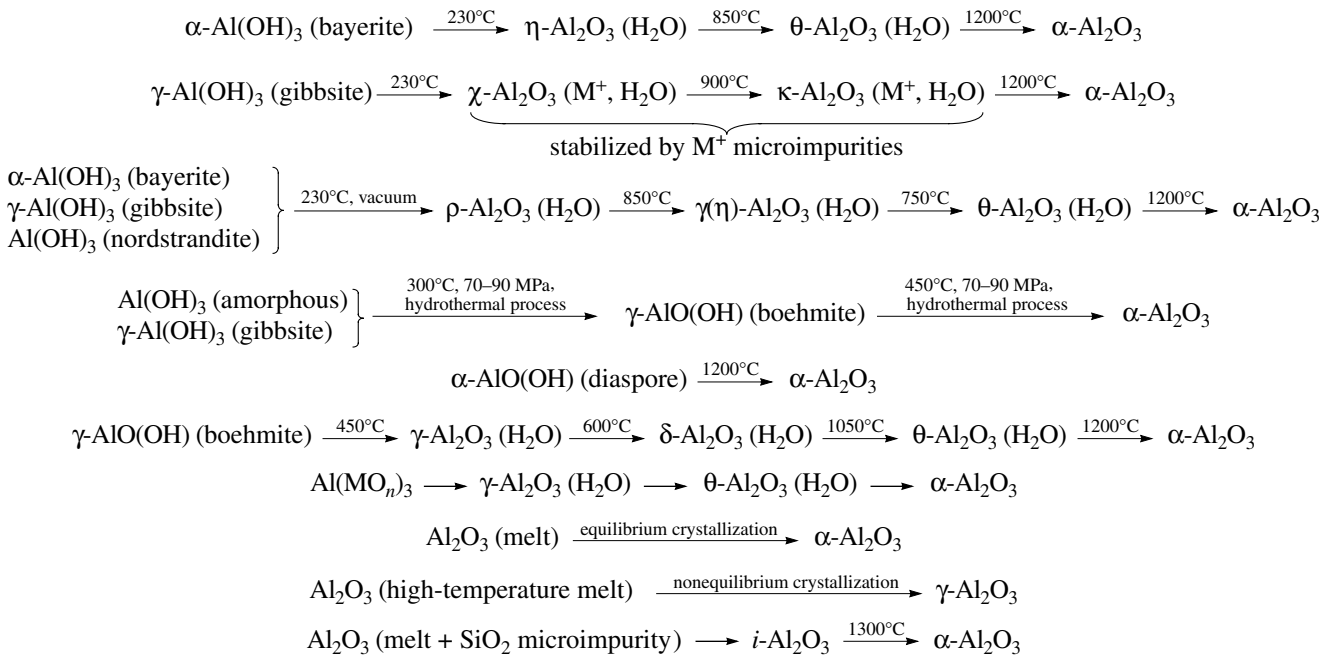

Fig. 1. Schemes of transformations resulting in various crystalline phases of alumina.

0020-1685/05/4105-0460

to 10 MPa, Toropov *et al.* [21] obtained nanocrystalline (30–80 nm) α-Al_2O_3 (Fig. 2). In addition, they obtained a new form of α-Al_2O_3, designated α-Al_2O_3–KI, and so-called "autoclave" γ-Al_2O_3, forming under hydrothermal conditions (400–500°C, 10–15 MPa). The phase diagrams in Fig. 2, though similar at low pressures, have a number of fundamental distinctions, in particular those associated with the possibility of γ-Al_2O_3 formation under hydrothermal conditions [21] and the α-Al_2O_3 stability region.

In this context, it is of interest to investigate aluminum hydroxide dehydration both theoretically and experimentally, especially with application to the preparation of α-Al_2O_3 nanoparticles.

THEORETICAL ANALYSIS

In thermodynamic calculations, we considered aluminum hydroxide in a crystalline ($Al(OH)_3$(cr), hydrargillite) or amorphous ($Al(OH)_3$(am)) state as the precursor to Al_2O_3. We analyzed four $Al(OH)_3$ dehydration schemes:

$$Al(OH)_3(am) \longrightarrow AlOOH\ (boehmite) \begin{cases} \nearrow\ \alpha\text{-}Al_2O_3 \\ \searrow\ \gamma\text{-}Al_2O_3 \end{cases}, \quad (1)$$

$$Al(OH)_3(cr) \longrightarrow AlOOH\ (boehmite) \begin{cases} \nearrow\ \alpha\text{-}Al_2O_3 \\ \searrow\ \gamma\text{-}Al_2O_3 \end{cases}, \quad (2)$$

$$Al(OH)_3(am) \longrightarrow AlOOH\ (diaspore) \begin{cases} \nearrow\ \alpha\text{-}Al_2O_3 \\ \searrow\ \gamma\text{-}Al_2O_3 \end{cases}, \quad (3)$$

$$Al(OH)_3(cr) \longrightarrow AlOOH\ (diaspore) \begin{cases} \nearrow\ \alpha\text{-}Al_2O_3 \\ \searrow\ \gamma\text{-}Al_2O_3 \end{cases}. \quad (4)$$

The calculation results were used to construct the general *p–t* phase diagram (Fig. 2), which is in reasonable agreement with the experimental data reported in [21, 23]. The only significant distinction is that the experimental *p–t* phase diagrams contain a γ-AlOOH (boehmite) stability region, whereas, according to the thermodynamic calculations, the most stable form of aluminum oxyhydroxide throughout its phase region is α-AlOOH (diaspore), with the implication that the α-AlOOH (diaspore) ⟶ γ-AlOOH (boehmite) transformation is thermodynamically implausible at any temperatures and pressures. The likely reason is that hydrargillite conversion into boehmite,

$$\gamma\text{-}Al(OH)_3 \xrightarrow{-H_2O} \gamma\text{-}AlOOH$$

is kinetically more favorable than diaspore formation since the former requires no significant structural

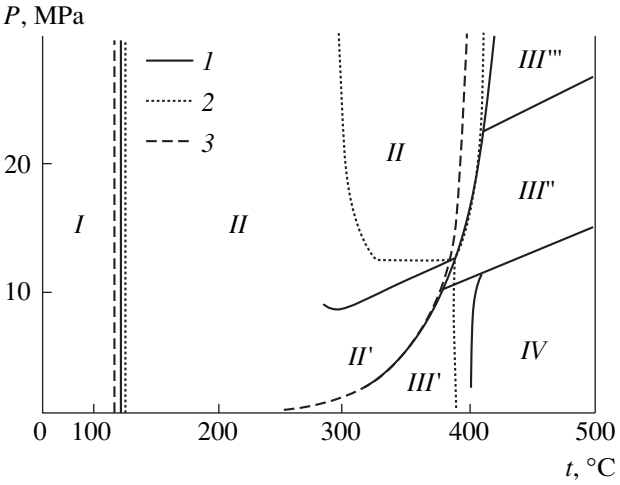

Fig. 2. *p–t* phase diagrams of the Al_2O_3–H_2O system: (*1*, *2*) experimental data from [21, 24], respectively; (*3*) calculation results; (*I*) $Al(OH)_3$ (hydrargillite), (*II*) stability region of diaspore, (*II'*) metastable boehmite phase region [21], (*III* = *III'* + *III''* + *III'''*) α-Al_2O_3 stability region (calculation results and experimental phase-diagram data from [24]), (*III'*) α-$Al_2O_3^*$ (nanocrystalline), (*III''*) α-Al_2O_3 (KI form), (*III'''*) α-Al_2O_3, (*IV*) γ-Al_2O_3 (autoclave alumina) according to the phase diagram in [21] and calculated α-Al_2O_3 stability region.

changes and, hence, is a fast reaction in terms of Buerger's classification [24]. In region *II'* (Fig. 2), boehmite formation is possible in unsaturated vapor. According to thermodynamic calculations, in the range 300–350°C the dehydration reaction

$$2\gamma\text{-}AlOOH \xrightarrow{-H_2O} \gamma\text{-}Al_2O_3$$

may occur, but γ-AlOOH under these conditions is unstable toward hydration:

$$\gamma\text{-}Al_2O_3 + H_2O \longrightarrow 2\alpha\text{-}AlOOH.$$

For this reason, the stable phase in region *III* at the pressures and temperatures in question is α-AlOOH.

Given that the calculated *p–t* phase boundary between diaspore and α-Al_2O_3 is in excellent agreement with the experimental data on the *p–t* phase region of α-Al_2O_3 formation (according to the experimental data, α-Al_2O_3 is formed from γ-AlOOH), it is reasonable to assume that α-Al_2O_3 formation from boehmite involves the γ-AlOOH ⟶ α-AlOOH transformation.

Note also that the calculation results suggest that, in the course of aluminum hydroxide dehydration in the temperature range where the formation of α-Al_2O_3 (200–450°C) and γ-Al_2O_3 (300–500°C) is thermodynamically plausible at pressures below 10 MPa, the equilibrium nucleus size of α- and γ-Al_2O_3 is rather small (5–20 nm) (Fig. 3), and the two polymorphs are

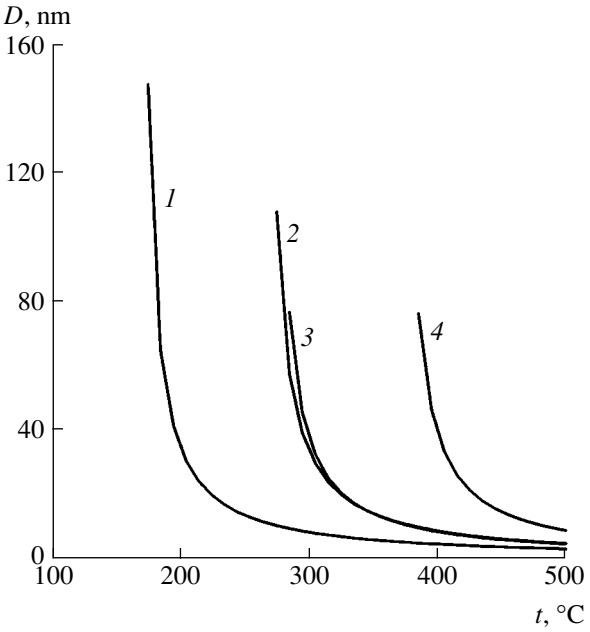

Fig. 3. Equilibrium nucleus size of Al_2O_3 as a function of process temperature: (*1*) γ-AlOOH ⟶ α-Al_2O_3 (2 MPa), (*2*) γ-AlOOH ⟶ α-Al_2O_3 (70 MPa), (*3*) γ-AlOOH ⟶ γ-Al_2O_3 (2 MPa), (*4*) γ-AlOOH ⟶ γ-Al_2O_3 (70 MPa).

likely to form by the fluctuation nucleation mechanism. Raising the pressure considerably increases the equilibrium nucleus size of γ-Al_2O_3, whereas that of α-Al_2O_3 remains virtually constant at 10–15 nm, which makes γ-Al_2O_3 formation by the fluctuation nucleation mechanism essentially impossible. This conclusion is supported by experimental data: analysis of the *p–t* phase diagram of the Al_2O_3–H_2O system (Fig. 2) [21] indicates that autoclave γ-Al_2O_3 can only form at pressures below 10–15 MPa. Note that, according to thermodynamic analysis results, γ-Al_2O_3 forming under hydrothermal conditions is unstable and must convert to α-Al_2O_3.

Thus, thermodynamic analysis (Figs. 2, 3) suggests that Al_2O_3 particles less than 100 nm in size can be prepared by any dehydration scheme at temperatures from 150 to 500°C and pressures from 0.1 to 70 MPa. At the same time, the formation of α-Al_2O_3 nanocrystals is most likely under hydrothermal conditions at 200–390°C and 2–10 MPa (Figs. 2, 3).

EXPERIMENTAL

It is of interest to examine the capabilities of hydrothermal synthesis for the preparation of α-Al_2O_3 nanoparticles because, as shown in the case of nanoparticulate ZrO_2 [25–28], hydrothermal processes yield isolated nanoparticles rather uniform in size. In our experiments, we used crystalline (hydrargillite) and x-ray amorphous aluminum hydroxides precipitated by adding an analytical-grade ammonium hydroxide solution to an 1 M analytical-grade aluminum chloride solution. The starting materials, differing not only in the structure of the $Al(OH)_3$ molecule but also in microstructure (Fig. 4), were treated isothermally at 250–500°C and 10–100 MPa in different hydrothermal environments: distilled water and aqueous solutions of NaF (0.5–1 wt %), NaOH (1–10 wt %), and Na_2CO_3 (0.5–1 wt %). The reaction time was varied from 30 min to 144 h. The reaction system had the form of a dilute suspension with a solid : liquid ratio of 1 : 50 to 1 : 100. According to earlier studies [29–32], mechanical activation of starting materials notably facilitates hydro-

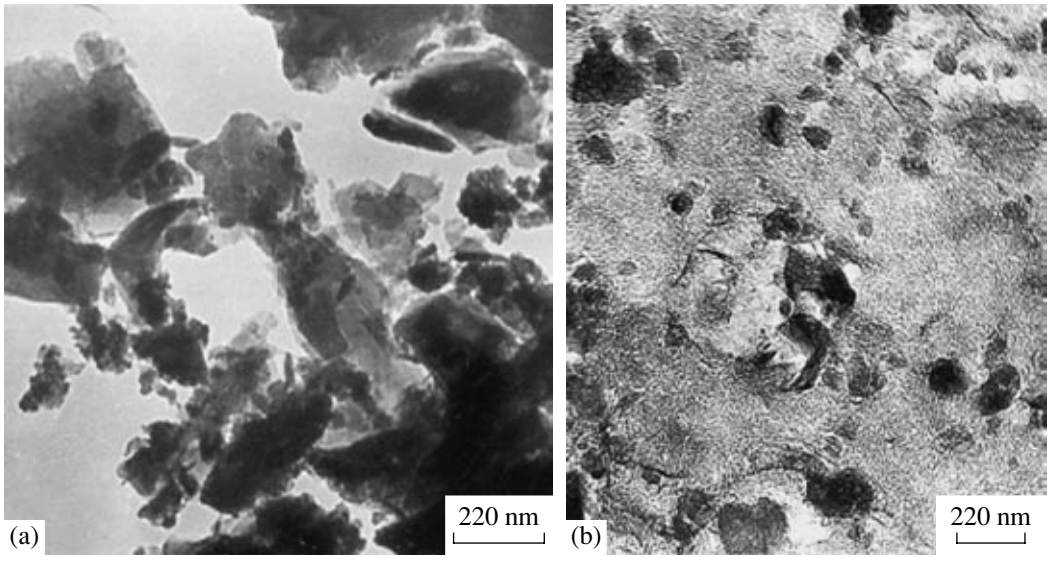

Fig. 4. Starting materials for hydrothermal synthesis: (a) crystalline $Al(OH)_3$ (hydrargillite), (b) amorphous $Al(OH)_3$.

thermal transformations in water vapor and enhances the structural perfection of the reaction product. In view of this, some of the reaction mixtures were sonicated at 22 MHz for 5–30 min to disaggregate the particles and ensure a uniform distribution of the particulate material over the hydrothermal solution.

Phase composition was determined on a DRON-3 x-ray diffractometer (scan step of 0.1°(2θ), counting time of 2 s per data point, CuK_α radiation). Microstructures were examined on an MIN-8 optical microscope and EM-125 transmission electron microscope (TEM) operated at 75 kV. TEM specimens were prepared by dispersing the powder in acetone for 5 min and spreading a drop of the suspension over a carbon support film.

RESULTS AND DISCUSSION

Detailed physicochemical characterization of hydrothermal reaction products revealed the following scheme of dehydration processes at elevated pressures:

$$\left.\begin{matrix}\text{Al(OH)}_3\text{(cr)}\\ \text{Al(OH)}_3\text{(am)}\end{matrix}\right\} \longrightarrow \gamma\text{-AlOOH (boehmite)} \longrightarrow \alpha\text{-Al}_2\text{O}_3.$$

Hydrothermal treatment of amorphous aluminum hydroxide in distilled water and NaOH and NaF solutions at temperatures from 250 to 300°C and pressures from 10 to 70 MPa yields only boehmite (γ-AlOOH) even at a reaction time as long as 144 h. This finding lends support to the above conclusions drawn from earlier reported experimental data and the calculated phase diagram of the Al_2O_3–H_2O system. Although the equilibrium phase in the temperature range in question is α-AlOOH (diaspore), hydrothermal treatment converts amorphous $Al(OH)_3$ to γ-AlOOH, presumably because the nucleation centers in amorphous $Al(OH)_3$ are similar in structure to γ-AlOOH, as is hydrargillite. After hydrothermal treatment of amorphous aluminum hydroxide at 450°C for 4 h, the reaction product contains about 50% α-Al_2O_3 (Fig. 5). After 24 h of treatment, the product is phase-pure α-Al_2O_3, rather than γ-Al_2O_3, a structural analog of boehmite, forming from γ-AlOOH during heat treatment in air. The likely reason is that, at 450°C, the ions on the surface of γ-AlOOH particles have increased mobility, which accelerates the rate of dissolution/crystallization processes, structural changes, equilibrium nucleation as a result of fluctuation effects, and other processes. This, in turn, leads to nucleation of α-Al_2O_3, an equilibrium phase under the conditions in question, rather than γ-Al_2O_3, a structural analog of boehmite.

The composition of the hydrothermal solution has little or no effect on the dehydration rate of $Al(OH)_3$. At the same time, compositional changes may slow down boehmite (γ-AlOOH) dehydration. This seems to be associated with the stabilization of oxyhydroxide species in the presence of alkali-metal cations by virtue of the formation of stable compounds, such as $MAlO_2$, which can be thought of as salts of metaaluminic acid, H–O–Al=O.

The use of crystalline aluminum hydroxide, γ-$Al(OH)_3$ (hydrargillite), as the starting material in the hydrothermal process causes no significant changes in the sequence of transformations compared to amorphous $Al(OH)_3$. Note however that, according to the data obtained at 450°C and 70 MPa, the dehydration rate of crystalline $Al(OH)_3$ is notably faster than that of x-ray amorphous aluminum hydroxide (Figs. 5, 6). The likely explanation for the faster rate of α-Al_2O_3 formation from crystalline $Al(OH)_3$ is that the crystalline material consists of larger particles, and the reaction

$$\gamma\text{-Al(OH)}_3 \xrightarrow{-\text{H}_2\text{O}} \gamma\text{-AlOOH},$$

accompanied by no significant structural changes, leads to the formation of larger γ-AlOOH particles as compared to the amorphous starting material. Accordingly, the overall process

$$\gamma\text{-Al(OH)}_3 \xrightarrow{-\text{H}_2\text{O}} \gamma\text{-AlOOH} \xrightarrow{-\text{H}_2\text{O}} \alpha\text{-Al}_2\text{O}_3$$

yields larger α-Al_2O_3 particles.

Thus, the overall rate of α-Al_2O_3 formation is faster at larger particle sizes of the starting material and intermediate reaction product. Note that experimental data

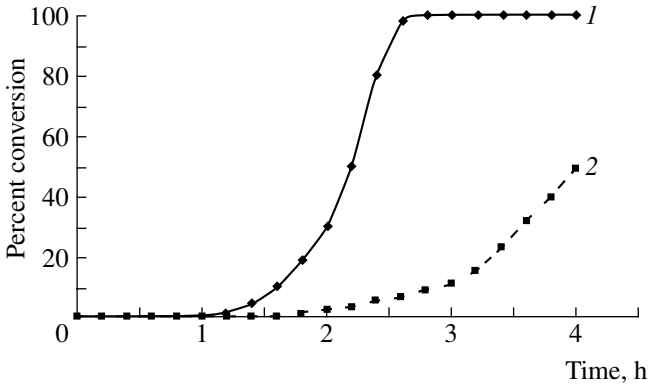

Fig. 5. Dehydration kinetics of (*1*) crystalline and (*2*) amorphous aluminum hydroxides under hydrothermal conditions at 450°C and 70 MPa (microscopic examination results).

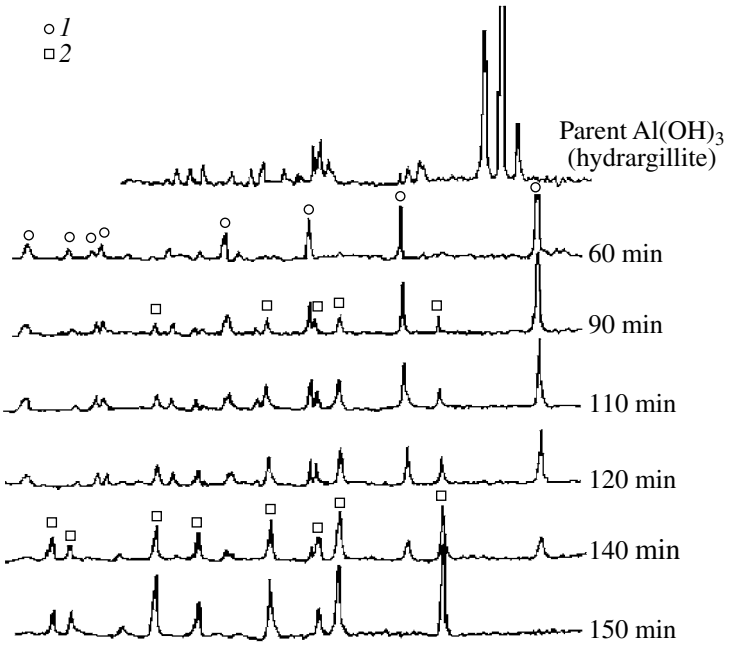

Fig. 6. X-ray diffraction patterns from the products of the hydrothermal treatment of crystalline aluminum hydroxide (hydrargillite) at 450°C and 70 MPa: (*1*) γ-AlOOH, (*2*) α-Al_2O_3.

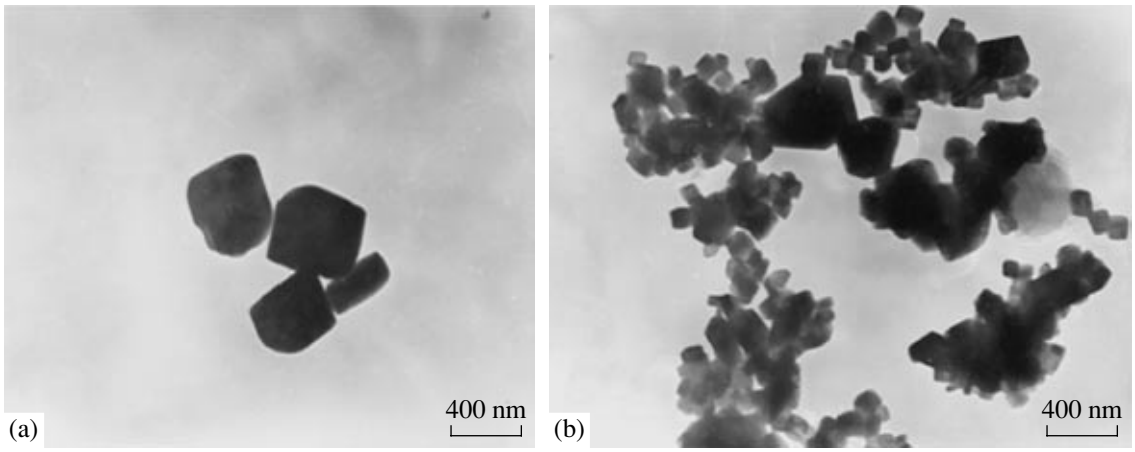

Fig. 7. TEM micrographs of α-Al_2O_3 crystals prepared by hydrothermal treatment of (a) hydrargillite and (b) amorphous $Al(OH)_3$ for 4 h at 450°C and 70 MPa.

confirm the conclusion that α-Al_2O_3 crystals prepared by the hydrothermal treatment of hydrargillite are larger than those prepared from amorphous $Al(OH)_3$ (Fig. 7).

In addition to crystalline and amorphous $Al(OH)_3$, we performed hydrothermal treatment of γ-Al_2O_3. The results lead us to conclude that, under hydrothermal conditions, α-Al_2O_3 is formed not through the direct transformation

$$\gamma\text{-}Al_2O_3 \longrightarrow \alpha\text{-}Al_2O_3,$$

but through the two-step process

$$\gamma\text{-}Al_2O_3 \xrightarrow{+H_2O} \gamma\text{-AlOOH} \xrightarrow{-H_2O} \alpha\text{-}Al_2O_3.$$

One possible explanation is that the hydration rate is substantially faster than the rate of the γ-Al_2O_3 ⟶ α-Al_2O_3 structural transition, first, because boehmite formation in the range 150–400°C is thermodynamically more favorable and, second, because the hydration process involves no drastic changes in the nearest neighbor environment of the Al ion (in contrast to the

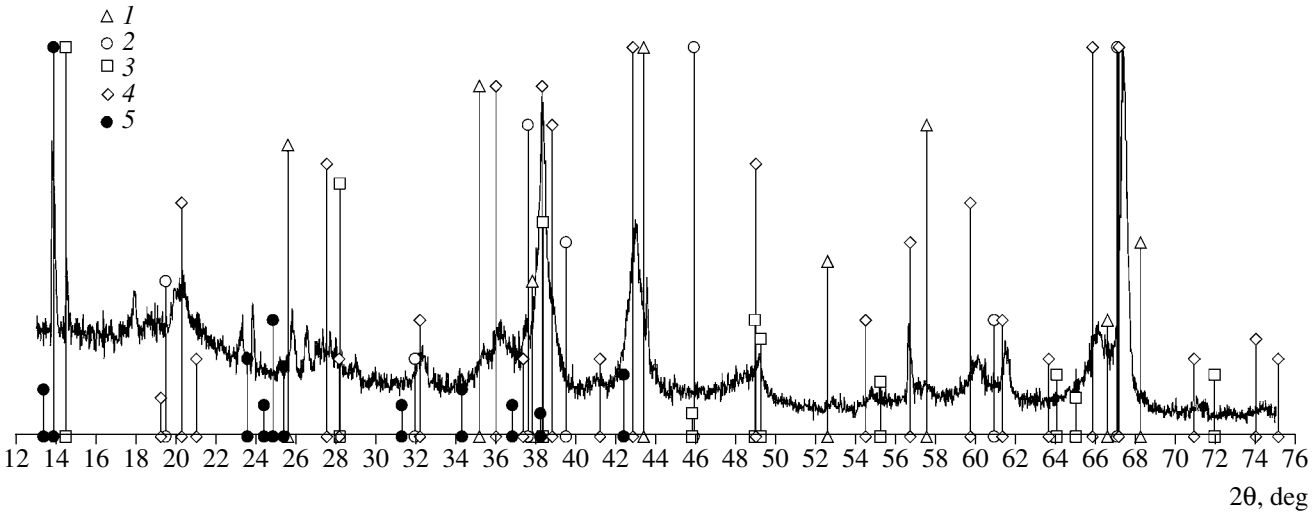

Fig. 8. X-ray diffraction pattern of $Al(OH)_3$ after hydrothermal treatment at 475°C and 2 MPa for about 5 h: (*1*) α-Al_2O_3, (*2*) γ-Al_2O_3, (*3*) γ-AlOOH, (*4*) $(Al_2O_3)_4 \cdot H_2O$, (*5*) $AlCl(OH)_2 \cdot 2H_2O$.

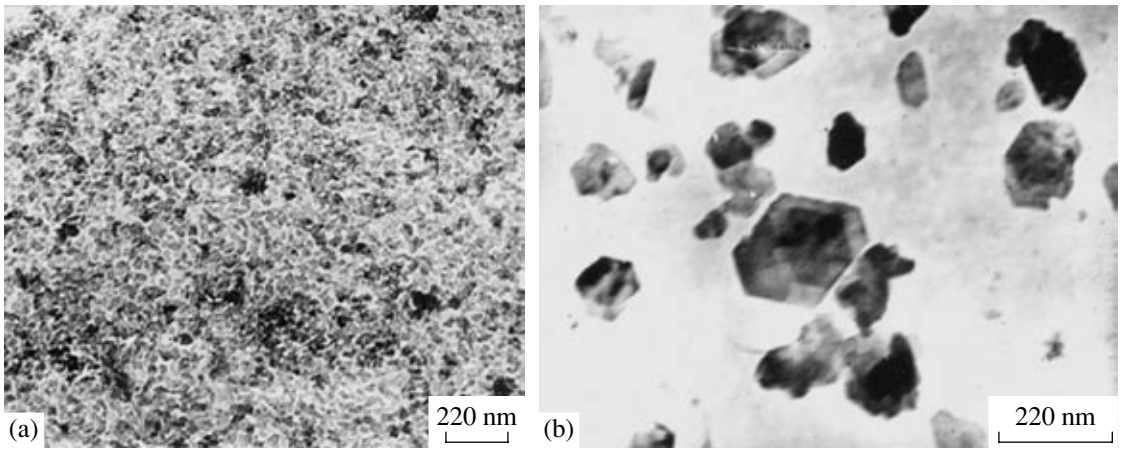

Fig. 9. TEM micrographs of particles obtained by hydrothermal treatment of amorphous $Al(OH)_3$ at 2 MPa for 5 h: (a) 400°C, (b) 475°C.

γ-$Al_2O_3 \longrightarrow \alpha$-$Al_2O_3$ transition) owing to the structural similarity between γ-Al_2O_3 and γ-AlOOH and must, therefore, occur rapidly [24].

The experimental phase-diagram data reported by Toropov *et al.* [21] for aluminum hydroxide and the present thermodynamic calculations (Fig. 2) led us to assume that the metastable phase γ-Al_2O_3 could be obtained under hydrothermal conditions at $t > 400$°C and $p < 10$ MPa. In connection with this, we examined the pressure effect on the dehydration of amorphous aluminum hydroxide. The results demonstrate that varying the pressure in the range 10–90 MPa has little or no effect on the dehydration process. At the same time, after short-term (5 h) treatment at 475°C and pressures below 10 MPa the x-ray pattern showed, in addition to peaks from boehmite and α-Al_2O_3, peaks attributable to a number of Al compounds: Al_2O_3 polymorphs and oxyhydroxides (Fig. 8). It seems likely that reducing the vapor pressure reduces the recrystallization rate and, therefore, the equilibration rate of the system. In such a situation, different oxyhydroxides and alumina polymorphs may coexist: from boehmite, rapidly forming from $Al(OH)_3$, to the equilibrium phase α-Al_2O_3. Note that the presence of nonequilibrium alumina polymorphs at relatively low water vapor pressures can be accounted for by the reduced hydration rate. Thus, it is reasonable to expect that a reduction in recrystallization and hydration rates, accompanied by an increase in dehydration rate by virtue of the decrease in water pressure in the autoclave, leads to the formation (and existence for a relatively long time) of different nonequilibrium and ultrafine aluminas, as confirmed by the present experimental data.

Below 475°C (350 and 400°C), hydrothermal treatment at 2 MPa yields only γ-AlOOH. Thus, thermodynamic calculations and experimental results demonstrate that the mechanism of $Al(OH)_3$ dehydration depends on the temperature and pressure in the autoclave.

In contrast to the decomposition of zirconium hydroxide (oxyhydroxide), resulting in the formation of ZrO_2 nanoparticles [25–28], the relatively slow dehydration rate of aluminum oxyhydroxide in comparison with the recrystallization rate leads to the formation of α-Al_2O_3 particles ranging in size from tens to hundreds of nanometers (Fig. 9). The present results suggest that, to increase the percentage of nanometer-sized particles, it is necessary to reduce the recrystallization rate and increase the dehydration rate of γ-AlOOH. At the same time, our results indicate that reducing the pressure may lead to the formation of nonequilibrium alumina polymorphs. Presumably, this can be avoided by using α-AlOOH (diaspore) as the starting material, because this oxyhydroxide is similar in structure to the equilibrium form of alumina, α-Al_2O_3.

CONCLUSIONS

Thermodynamic analysis of phase equilibria in the Al_2O_3–H_2O system at temperatures from 120 to 380°C and pressures from 1 to 70 MPa indicates that the stable form of aluminum oxyhydroxide is α-AlOOH (diaspore). Therefore, γ-AlOOH (boehmite), which commonly appears in experimental phase diagrams, is a nonequilibrium phase in these temperature and pressure ranges.

Experimental data and theoretical analysis demonstrate that the mechanisms of $Al(OH)_3$ dehydration and α-Al_2O_3 formation under hydrothermal conditions depend strongly on pressure.

The rate of α-Al_2O_3 formation under hydrothermal conditions is shown to depend on the structure of the parent aluminum hydroxide.

We established the hydrothermal conditions under which α-Al_2O_3 nanoparticles are likely to form. In particular, our results indicate that reducing the pressure in the hydrothermal system increases the percentage of α-Al_2O_3 particles less than 100 nm in size.

ACKNOWLEDGMENTS

This work was supported by the Russian Foundation for Basic Research, grant no. 03-03-32402.

REFERENCES

1. Kazakov, S.V., Sokolov, A.N., Tsiporina, S.Z., *et al.*, Aluminum Oxide with Mullite Structure, *Izv. Akad. Nauk SSSR, Neorg. Mater.*, 1988, vol. 24, no. 12, pp. 2010–2013.
2. Kiselev, V.F. and Krylov, O.V., *Adsorbtsionnye protsessy na poverkhnosti poluprovodnikov i dielektrikov* (Adsorption Processes on Semiconductor and Dielectric Surfaces), Moscow: Nauka, 1978.
3. Dzis'ko, V.A., Karnaukhov, A.P., and Tarasova, D.V., *Fiziko-khimicheskie osnovy sinteza okisnykh katalizatorov* (Physicochemical Principles behind the Synthesis of Oxide Catalysts), Novosibirsk: Nauka, 1978.
4. Kiselev, A.V. and Lygin, V.I., *Infrakrasnye spektry poverkhnostnykh soedinenii* (Infrared Spectra of Surface Species), Moscow: Nauka, 1972.
5. Lippens, B.C. and Steggerda, I.I., Active Alumina, *Physical and Chemical Aspects of Adsorbents and Catalysts*, Linsen, B.G., Ed., London: Academic, 1970. Translated under the title *Stroenie i svoistva adsorbentov i katalizatorov*, Moscow: Mir, 1973, pp. 190–230.
6. Chukin, G.D. and Seleznev, Yu.L., Mechanism of the Thermal Decomposition of Boehmite and a Structural Model of Aluminum Oxide, *Kinet. Katal.*, 1989, vol. 30, no. 1, pp. 69–77.
7. Mardilovich, P.P., Trokhimets, A.I., Zaretskii, M.V., and Kupchenko, G.G., IR Spectroscopic Study of Bayerite and Hydrargillite Dehydration, *Zh. Prikl. Spektrosk.*, 1985, vol. 42, no. 6, pp. 959–966.
8. *Catalyst Supports and Supported Catalysts: Theoretical and Applied Concepts*, Stiles, A.B., Ed., Boston: Butterworths, 1988. Translated under the title *Nositeli i nanesennye katalizatory. Teoriya i praktika*, Moscow: Khimiya, 1991.
9. Kalinina, A.M., On the Polymorphism and Thermal Transformation of Aluminum Oxide, *Zh. Neorg. Khim.*, 1959, vol. 4, no. 6, pp. 1261–1269.
10. Rubinshtein, A.M., Slovetskaya, K.I., Akimov, V.M., *et al.*, Polymorphism and Catalytic Performance of Al_2O_3, *Izv. Akad. Nauk SSSR, Ser. Khim.,* 1960, no. 1, pp. 31–37.
11. Sasvari, K. and Zalai, A., The Crystal Structure and Thermal Decomposition of Alumina Hydrates as Regarded from the Point of View of Lattice Geometry, *Acta Geol. Hung.*, 1957, vol. 4, pp. 415–465.
12. Dzis'ko, V.A. and Ivanova, A.S., Basic Processes for the Preparation of Active Alumina, *Izv. Sib. Otd. Akad. Nauk SSSR, Ser. Khim. Nauk*, 1985, vol. 15, no. 5, pp. 110–119.
13. Krivoruchko, O.P., Buyanov, R.A., Fedotov, M.A., and Plyasova, M.N., Formation Mechanisms of Bayerite and Pseudoboehmite, *Zh. Neorg. Khim.,* 1978, vol. 23, no. 7, pp. 1796–1803.
14. Shkrabina, R.A., Moroz, E.M., and Levitskii, E.A., Polymorphous Transformations of Aluminum Oxides and Hydroxides, *Kinet. Katal.*, 1981, vol. 22, no. 5, pp. 1293–1299.
15. Yanagida, H. and Yamaguchi, G., Thermal Effect on the Lattices of γ- and η-Aluminium Oxide, *Bull. Chem. Soc. Jpn.*, 1964, vol. 37, no. 8, pp. 1229–1230.
16. Lippens, B.C. and De Boer, J.H., Study of Phase Transformations during Calcinations of Aluminium Hydroxides by Selected Area Electron Diffraction, *Acta Crystallogr.,* 1964, vol. 17, pp. 1312–1321.
17. Saalfeld, H., Structure Phases of Dehydrated Gibbsite, *React. Solids*, 1961, pp. 310–316.

18. Ryabov, N.A., Kozhina, I.I., and Kozlov, I.L., Effect of Preparation Conditions on the Polymorphic Transformations of Aluminum Oxide, *Zh. Neorg. Khim.*, 1970, vol. 15, no. 3, pp. 602–606.

19. Levin, I. and Brandon, D., Metastable Alumina Polymorphs: Crystal Structures and Transition Sequences, *J. Am. Ceram. Soc.*, 1998, vol. 81, no. 8, pp. 1995–2012.

20. Sharma, P.K., Jilavi, M.H., Bugard, D., *et al.*, Hydrothermal Synthesis of Nanosize α-Al_2O_3 from Seeded Aluminum Hydroxide, *J. Am. Ceram. Soc.,* 1998, vol. 81, no. 10, pp. 2732–2734.

21. Toropov, N.A., Barzakovskii, V.P., Lapin, V.V., and Kurtseva, N.N., *Diagrammy sostoyaniya silikatnykh sistem: Spravochnik* (Phase Diagrams of Silicate Systems: A Handbook), Leningrad: Nauka, 1965, issue 1, p. 546.

22. Laubengayer, A.W. and Weiss, R.S., *J. Am. Chem. Soc.,* 1943, vol. 65, no. 2, p. 250.

23. Erwin, G. and Osborn, E.F., *J. Geol.*, 1951, vol. 59, no. 4, p. 381.

24. Buerger, M.J., Polymorphism and Phase Transformation, *Fortschr. Miner.*, 1961, vol. 39, pp. 9–24.

25. Pozhidaeva, O.V., Korytkova, E.N., Drozdova, I.A., and Gusarov, V.V., Effect of Hydrothermal Synthesis Conditions on the Phase State and Particle Size Ultrafine Zirconia, *Zh. Obshch. Khim.*, 1999, vol. 69, no. 8, pp. 1265–1270.

26. Pozhidaeva, O.V., Korytkova, E.N., Romanov, D.P., and Gusarov, V.V., Formation of Zirconia Nanocrystals in Various Hydrothermal Systems, *Zh. Obshch. Khim.*, 2002, vol. 72, no. 6, pp. 910–914.

27. Shigeyuki Somiya and Tokuji Akiba, Hydrothermal Zirconia Powders: A Bibliography, *J. Eur. Ceram. Soc.*, 1999, no. 19, pp. 81–87.

28. Burukhin, A.A., Oleinikov, N.N., Churagulov, B.R., *et al.*, Synthesis of Nanocrystalline Zirconia in Hydrothermal and Supercritical Solutions, *Vestn. Voronezh. Gos. Tekh. Univ., Ser. Materialoved.*, 1999, issue 1.5, pp. 19–24.

29. Avvakumov, E.G., *Mekhanicheskie metody aktivatsii khimicheskikh protsessov* (Mechanical Activation of Chemical Processes), Novosibirsk: Nauka, 1986.

30. *Mekhanokhimicheskii sintez v neorganicheskoi khimii* (Mechanochemical Synthesis in Inorganic Chemistry), Novosibirsk: Nauka, 1991.

31. Grigor'eva, T.F., Vorsina, I.A., Barinova, A.P., and Lyakhov, N.Z., Early Stages in Mechanochemical Activation of Kaolinite and Talc, *Neorg. Mater.*, 1996, vol. 32, no. 1, pp. 84–89 [*Inorg. Mater.* (Engl. Transl.), vol. 32, no. 1, pp. 75–79].

32. Danchevskaya, M.N., Ivakin, Yu.D., Murav'eva, G.P., and Zui, A.I., Transformation of Mechanically Activated Hydrargillite Exposed to High Temperatures and Water Vapor, *Vestn. Mosk. Univ., Ser. 2: Khim.*, 1997, vol. 38, no. 1, pp. 21–25.